

ANALYSIS OF THE TEMPERATURE OF A CIRCULAR
ELECTRODE

N. V. Pashatskii and S. V. Osovets

UDC 533.924

Results are presented of numerical computations of the temperature fields in the circular electrode of a plasmotron. Taken into account in the model proposed are the nonlinearity in the boundary conditions, the dependence of the electrode material properties on the temperature, the heat of phase transformation, etc.

Electrodes from graphite materials are utilized extensively in electric-arc units [1, 2], however, the temperature conditions for their operation have still been studied insufficiently. A model in which the cylindrical electrode geometry, the dependence of the coefficient of thermal diffusivity of the material on the temperature, the heat losses by radiation and evaporation for a material with external side and endface surfaces, and finite size of the heat source are taken into account in contrast to earlier papers [3], is used in the present investigation to compute the two-dimensional temperature field in a circular graphite electrode of a plasmotron.

The following assumptions are used in the analysis: changes in the electrode size due to erosion are insignificant, the heat flux is delivered just through the reference spot of the electric arcs on the electrode endface surface. Since thermal sources are surface sources, their action is taken into account in the boundary condition by giving the heat flux density q . Furthermore, it is assumed that the sources are "spread out" uniformly over a ring of width δ on the electrode endface. Such a passage from spots to a ring (arc path) is justified by the fact that arc spots are, as experiments show, in continuous motion near the middle of the circle on the endface surface. The spot diameter is $d_s = (2-3) \cdot 10^{-3}$ m.

The differential equation of heat conduction of a circular electrode has the following form in cylindrical coordinates

$$\frac{\partial T}{\partial \tau} = \frac{\partial}{\partial r} \left[a(T) \frac{\partial T}{\partial r} \right] + a(T) \frac{1}{r} \frac{\partial T}{\partial r} + \frac{\partial}{\partial z} \left[a(T) \frac{\partial T}{\partial z} \right]. \quad (1)$$

Equation (1) is solved under the following boundary conditions

$$\frac{\partial T}{\partial r} \Big|_{r=r_1} = hT, \quad (2)$$

$$\frac{\partial T}{\partial r} \Big|_{r=r_2} = \frac{1}{\rho c a(T)} [\sigma T^4 + v(\rho c T + L)], \quad (3)$$

$$\frac{\partial T}{\partial z} \Big|_{z=0} = \frac{1}{\rho c a(T)} [\sigma T^4 + v(\rho c T + L) - q], \quad (4)$$

$$T(r, l, \tau) = T_0,$$

$$T(r, z, 0) = T_0,$$

$$q = \frac{Q}{\pi \delta (r_1 + r_2)},$$

$$q = 0, \quad r_1 \leq r < \frac{r_1 + r_2 - \delta}{2} \quad \text{and} \quad \frac{r_1 + r_2 + \delta}{2} < r \leq r_2.$$

The quantity h in (2) governs just the convective heat elimination from the inner surface of the circular electrode since the heat losses by radiation from this surface are compensated by the incident radiation from the rod electrode. The value of h for a spiral flux

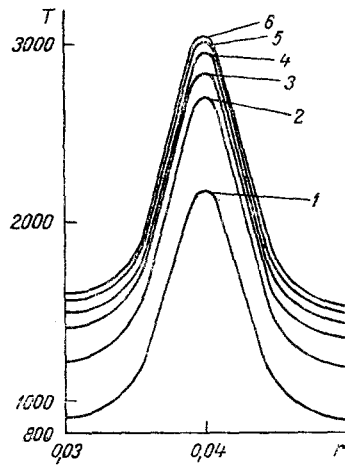


Fig. 1

Fig. 1. Temperature on the electrode endface: 1) $\tau = 10$ sec; 2) 20; 3) 30; 4) 40; 5) 50; 6) 60 sec.

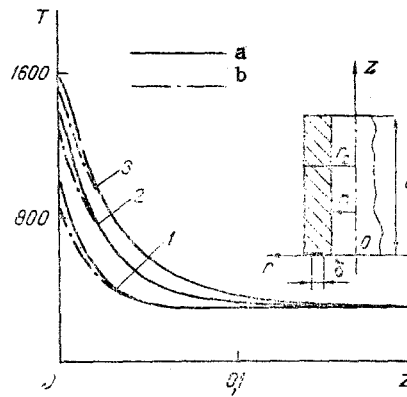


Fig. 2

Fig. 2. Temperature distribution over the electrode length: 1) $\tau = 10$; 2) 30; 3) 60 sec; a) $r = r_1$; b) $r = r_2$

is selected on the basis of data of [4].

Thermal radiation exerts resolving influence on the temperature of the electrode external surfaces, consequently we neglect heat convection for these surfaces.

The first component in the square brackets in conditions (3) and (4) describes the radiation process, and the second, the process of electrode material evaporation.

The product of the graphite density by its specific heat ρc is assumed constant and independent of the temperature [1]. A formula presented in [5]

$$a(T) = 3.64 \cdot 10^{-5} [\exp(375/T) - 1].$$

is used to compute the thermal diffusivity of graphite.

The dependence of the rate of graphite evaporation v on the temperature is found on the basis of data on evaporation in a vacuum [6] and has the following form

$$v = \frac{1.25 \cdot 10^{11} \exp(-92500/T)}{\sqrt{T}}.$$

Let us note that the results of computing v by means of this expression for temperatures of ~ 3000 K and above are in good agreement with experimental data on erosion [7] despite the fact that these latter were obtained at atmospheric pressure in air.

The values of the geometric and physical parameters in the computation were the following: $r_1 = 0.03$; $r_2 = 0.05$; $l = 0.2$; $\delta = 2.5 \cdot 10^{-3}$ m; $\rho = 1700$ kg/m³; $c = 2078$ (J/(kg·K)); $L = 2.14 \cdot 10^7$ J/kg (for C₃), $\sigma = 5.67 \cdot 10^{-8}$ W/(m²·K⁴), $T_0 = 293$ K. The thermal flux power from the arc in the electrode equals $2 \cdot 10^4$ W as in [3].

The method of alternate directions using an implicit finite-difference scheme of first-order accuracy in the time and of second-order accuracy in the space variable $\sim O(h_\tau, h_z^2, h_r^2)$ [8] was applied for numerical computations in this model. The computation was performed on a 8×40 ($r \times z$) mesh with the time step $h_\tau = 0.25$ sec, and the computation error was ± 20 K.

As was shown in [3], the stationary mode was achieved along the electrode length in approximately 5 min. In connection with the fact that we are interested principally in the temperature field on the endface working surface (and here the stationary mode is achieved, in practice, after 1-2 min), all the computations are performed for $\tau \leq 60$ sec.

It is seen from Fig. 1 that as was expected, an almost stationary state is set up after approximately 60 sec on the electrode working surface. The maximal value of the temperature is 3040 K.

The temperature on the side surfaces drops sharply in the direction towards the cold

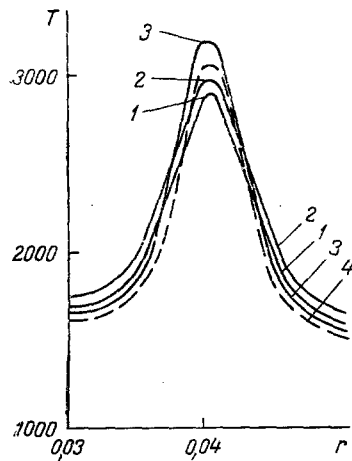


Fig. 3

Fig. 3. Electrode endface temperature for $\ell = 0.1$ m (1), $a = \text{const} = 12.5 \cdot 10^{-4}$ m²/sec (2), $v = 0$ (3); 4) fundamental model $\tau = 60$ sec.

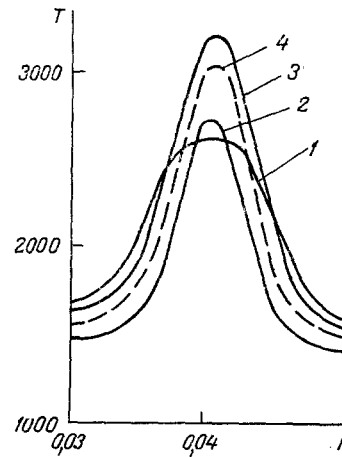


Fig. 4

Fig. 4. Endface surface temperature for $\delta = 7.5 \cdot 10^{-3}$ m (1), $Q = 15$ (2), $Q = 25$ kW (3); $\tau = 60$ sec; 4) fundamental model.

end of the electrode: diminished almost in half for $z \approx (0.1 - 0.2)\ell$ (Fig. 2). Despite the different boundary conditions on the outer and inner electrode surfaces, the temperatures of these surfaces differ slightly from each other ($\Delta T < 100$ K for $z = 0$), and the difference vanishes at distances $z \geq 0.1\ell$ from the working endface.

As the electrode length diminishes, the temperature maximum on the endface is reduced while the temperature on the electrode inner and outer edges increases somewhat (curve 1 in Fig. 3). The same pattern is observed if the graphite thermal diffusivity coefficient (in the 293-3000 K temperature range) is taken constant in the computations and equal to $12.5 \cdot 10^{-6}$ m²/sec. Finally, upon discarding the evaporation term in the conditions (3) and (4), the temperature grows noticeably as the source center is approached, and remains almost the same on the electrode edges as in the fundamental model.

Since the size of the source (the mean diameter of the reference spot) and its power depend on the operating mode of the plasma head, it is interesting to investigate the dependence of the electrode temperature on these factors also.

As the width δ of the arc path increases (from $2.5 \cdot 10^{-3}$ to $7.5 \cdot 10^{-3}$ m), which can correspond to transition to the stationary thermal state (heating) of the electrodes in practice, the temperature at the point of the maximum at the endface is reduced sharply (Fig. 4). Changes in the thermal source intensity (with $\pm 25\%$ limits) also exert significant influence on the temperature, especially at the center of the endface.

Therefore, the numerical experiment showed that the most essential factors governing the temperature field at a circular electrode endface are the thermal source intensity and size. The dependence of the thermal diffusivity coefficient on the temperature and evaporation of the material exert less influence on the electrode temperature.

The reduced computed, almost stationary, value of the temperature on the endface inner and outer edges ($T_{r_1} = 2064$, $T_{r_2} = 1849$ K, $z = 0$, $\tau = 150$ sec) as compared with experiment [3] ($T_{r_2} = 2200$ K) can be explained by the neglect of radial displacements of the arc spots caused by shunting in the model, which equilibrate the temperature on the electrode endface.

NOTATION

T , absolute temperature; r , radius; z ; longitudinal coordinate; a , thermal diffusivity coefficient, ρ , density; c , specific heat; L , heat of evaporation; σ , Stefan-Boltzmann constant; $h = \alpha/\kappa$, reduced heat elimination coefficient; κ , heat conduction coefficient; v , rate of material evaporation; and τ , time.

LITERATURE CITED

1. M. I. Rogailin and E. F. Chalykh, Handbook on Carbon Graphite Materials [in Russian], Leningrad (1974).
2. É. N. Marmer, Carbon-Graphite Materials [in Russian], Moscow (1973).
3. N. V. Pashatskii and V. N. Malkov, Inzh.-Fiz. Zh., 48, No. 6, 1012 (1985).
4. V. K. Shchukin and A. A. Khalatov, Heat Transform and Hydrodynamics of Spiral Flows in Axisymmetric Channels [in Russian], Moscow (1982).
5. V. S. Chirkin, Thermophysical Properties of Nuclear Engineering Materials [in Russian], Moscow (1968).
6. A. N. Nesmeyanov, Vapor Pressure of Chemical Elements [in Russian], Moscow (1961).
7. N. V. Pashatskii and E. A. Molchanov, Izv. Sib. Otd. Akad. Nauk SSSR, Ser. Tekh. Nauk, No. 8, Issue 2, 62-65 (1980).
8. A. A. Samarskii and E. S. Nikolaev, Methods of Solving Mesh Equations [in Russian], Moscow (1978).

ANALYSIS OF THE CORRECTNESS OF A TWO-TEMPERATURE COMPUTATION METHOD

I. V. Goncharov and V. L. Mikov

UDC 536.2.01

Two methods of determining the heat transfer coefficient between components are compared on the basis of an exact solution of a model problem.

A multitemperature method [1-4] whose general principles are elucidated in [1] is used extensively at this time to model heat transport processes in heterogeneous media (granular, laminar, fibrous). This approach is based on taking the average of the thermophysical parameters with respect to each component in a macrovolume element, which results in a system of interrelated heat conduction equations. The connection between the heat flux between the components and their mean temperatures for which the Henry law is utilized [1]

$$q_{ij}^* = \alpha(\bar{T}_i - \bar{T}_j) \quad (1)$$

must be established to close the system.

Two methods are known for determining α : the "correlation" [1] and the linear radial heat flux methods [4, 5]. The problem of analyzing the correctness of the methods to determine the heat transfer coefficient between components is posed in this paper.

Let us examine a model heat propagation problem in a bilaminar composite of regular structure under boundary conditions of the second kind. The representative section of the material is displayed in Fig. 1. The thermophysical characteristics of the material components are considered independent of the temperature. Then we can write for an isolated section element

$$\lambda_{zi} T_{i,zz} + \lambda_{xi} T_{i,xx} = c_i T_{i,t}, \quad i = 1, 2, \quad (2)$$

$$T_i(0, z, x) = 0, \quad (2a)$$

$$-\lambda_{zi} T_{i,z}|_{z=0} = q_0(t), \quad \lambda_{zi} T_{i,z}|_{z=n} = q_n(t), \quad (2b)$$

$$T_{i,x} = 0, \quad x = l_i, \quad (2c)$$

$$-\lambda_{x1} T_{1,x} = \lambda_{x2} T_{2,x}, \quad T_1 = T_2, \quad x = 0. \quad (2d)$$

1. Two-Temperature Theory. Let us introduce the concept of the mean temperature over

a section $\bar{T}_i = \frac{1}{l_i} \int_0^{l_i} T dx$. Then (2) can be converted into

$$\lambda_{zi} T_{i,zz} - c_i \bar{T}_{i,t} = \frac{(-1)^{i+1}}{l_i} q^*, \quad i = 1, 2,$$

Translated from Inzhenerno-Fizicheskii Zhurnal, Vol. 58, No. 2, pp. 311-316, February, 1990. Original article submitted August 2, 1988.